Geometric mass acquisition via a quantum metric: An effective-band-mass theorem for the helicity bands

M. Iskin
Department of Physics, Koç University, Rumelifeneri Yolu, 34450 Sarıyer, Istanbul, Turkey

(Received 20 March 2018; published 7 May 2019)

By fully taking into account the virtual interband processes along with the intraband ones, here we propose an effective-band-mass theorem that is suitable for a wide class of single-particle Hamiltonians exhibiting multiple energy bands. Then, for the special case of two-band systems, we show that the interband contribution to the effective band mass of a particle at a given quantum state is directly controlled by the quantum metric of the corresponding state. As an illustration, we consider a spin-orbit-coupled spin-$\frac{1}{2}$ particle and calculate its effective band mass at the band minimum of the lower helicity band. Independent of the coupling strength, we find that the bare mass m_0 of the particle jumps to $2m_0$ for the Rashba coupling and to $3m_0$ for the Weyl coupling. This geometric mass enhancement is a nonperturbative effect, uncovering the mystery behind the effective mass of the two-body bound states in the noninteracting limit. As a further illustration, we show that a massless Dirac quasiparticle acquires a linearly dispersing band mass (equivalent to the effective cyclotron mass up to a prefactor) with its momentum through the same mechanism.

DOI: 10.1103/PhysRevA.99.053603

I. INTRODUCTION

Depending on the physical context, the helicity of a particle may refer to the projection of its orbital and/or spin angular momentum into the direction of its center-of-mass motion, e.g., the helicity is said to be right (left) handed when the relevant quantities are aligned (antialigned). One of the central themes in a wide range of modern single-, two-, few-, or many-body physics problems is the so-called spin-orbit coupling (SOC), as it has found a plethora of interdisciplinary applications across atomic and molecular, particle, high-energy, nuclear, solid-state, and condensed-matter physics, spreading over many decades. A great deal of these problems involve a $(\mathbf{d}_\mathbf{k} \cdot \boldsymbol{\sigma})$-like $\mathbf{k}$-dependent Zeeman term in the equations of motion, where the motional degrees of freedom are described by some vector field $\mathbf{d}_\mathbf{k}$ that depends on the linear momentum $\mathbf{p} = \hbar\mathbf{k}$ through the wave vector $\mathbf{k}$ and $\boldsymbol{\sigma}$ is a vector of spin matrices corresponding to the spin or generally pseudospin (e.g., sublattice, hyperfine, and valley) degrees of freedom. For instance, the generic coupling $\hbar \sum_i \alpha_i k_i \sigma_i$ is widespread in physics literature, describing cold atoms in artificial non-Abelian gauge fields [1–11], Dirac electrons in low-energy excitations of graphene [12–14], and Dirac quasiparticles at the surface of three-dimensional topological insulators [15,16], organic quasi-two-dimensional materials [17], and artificial honeycomblike (e.g., optical [18], molecular [19], and microwave [20]) crystals.

Given the foremost importance of the spin-momentum coupling for the general physics community, here we develop a so-called effective-band-mass theorem for the helicity bands that is suitable for a wide class of single-particle Hamiltonians. Our theorem has two physically distinct components: In addition to the usual contribution coming from the intraband processes, there is a geometric contribution stemming from the virtual interband ones controlled by the quantum metric of the corresponding quantum state. As an illustration, first we consider a spin-orbit-coupled spin-$\frac{1}{2}$ particle and calculate its effective band mass at the band minimum of the lower helicity band. It turns out that the bare mass m_0 of the particle jumps to $2m_0$ for the Rashba coupling and to $3m_0$ for the Weyl coupling independently of the coupling strength, i.e., the geometric mass enhancement is a nonperturbative effect. Since the quantum metric effects are both rare and elusive in nature [21–36], the experimental verification of these predictions with the recently realized Rashba-like SOCs [8–11] would be an important leap towards the geometric and topological interpretations of quantum mechanics [37–39]. As a further illustration, we then apply the theorem to a massless Dirac quasiparticle, showing that the acquired geometric band mass of the particle disperses linearly with its momentum.

It is important to emphasize that the quantum metric contribution to the effective band mass of a single particle revealed in this paper is distinct from our recent findings on a counterpart effect on the effective mass of many-body (Cooper pairs) as well as two-body (molecular) bound states throughout the BCS-BEC crossover in superfluid Fermi gases [33,34]. These previous works revealed that, through dressing the effective mass of the relevant bound state, the quantum metric governs not only the superfluid density of some flat-band [31,32] and two-band [33,35] Fermi superfluids exhibiting nontrivial quantum geometry, but also many other observables including the sound velocity and spin susceptibility [36]. Unlike all of these previous works on Fermi superfluids where the quantum metric is integrated over $\mathbf{k}$ space with some additional weight factors, this work paves a direct way towards measuring a local and nonperturbative quantum metric effect on either pseudo-spin-$\frac{1}{2}$ Fermi [8,9] or Bose [10,11] gases, independently of the particle statistics.

II. EFFECTIVE-BAND-MASS THEOREM FOR MULTIBAND HAMILTONIANS

Having multiple bands in mind, we consider a generic band structure that is determined by the wave equation $H_{\mathbf{k}}|n\mathbf{k}\rangle = \varepsilon_{n\mathbf{k}}|n\mathbf{k}\rangle$, where $H_{\mathbf{k}}$ is the single-particle Hamiltonian density in reciprocal space and $|n\mathbf{k}\rangle$ and $\varepsilon_{n\mathbf{k}}$ denote, respectively, the corresponding energy eigenstates and eigenvalues. Here the quantum states are labeled by the band index n and wave vector $\mathbf{k}$. In the presence of such a multiband setting, the conventional wisdom [40] for the definitions of the effective band velocity $\mathbf{v}_{n\mathbf{k}}$ and effective-band-mass tensor $\mathbb{M}_{n\mathbf{k}}$ of a particle is such that they are determined by the coefficients of the linear and quadratic terms in the small-$\mathbf{q}$ expansion

$$\varepsilon_{n,\mathbf{k}+\mathbf{q}} = \varepsilon_{n\mathbf{k}} + \hbar\sum_i v_{n\mathbf{k}}^i q_i + \frac{\hbar^2}{2}\sum_{ij}\left[\mathbb{M}_{n\mathbf{k}}^{-1}\right]^{ij} q_i q_j + \cdots .$$

Thus, both the components $v_{n\mathbf{k}}^i$ of the velocity and the principal values $M_{n\mathbf{k}}^P$ of the mass tensor may have a strong dependence on $\mathbf{k}$ that is controlled by the microscopic details of a given system.

Noting that $\varepsilon_{n,\mathbf{k}+\mathbf{q}}$ is an energy eigenvalue of $H_{\mathbf{k}+\mathbf{q}}$, one can simply obtain these effective band parameters through perturbation theory. For this purpose, we first perform a small-$\mathbf{q}$ expansion of the Hamiltonian $H_{\mathbf{k}+\mathbf{q}} = H_{\mathbf{k}} + \sum_i q_i\partial H_{\mathbf{k}}/\partial k_i + \frac{1}{2}\sum_{ij} q_i q_j \partial^2 H_{\mathbf{k}}/\partial k_i\partial k_j + \cdots$ and then treat all of the $\mathbf{q}$-dependent terms as a perturbative correction $V_{\mathbf{kq}}$ to the unperturbed Hamiltonian $H_{\mathbf{k}}$, i.e., $H_{\mathbf{k}+\mathbf{q}} = H_{\mathbf{k}} + V_{\mathbf{kq}}$, in the small-$\mathbf{q}$ limit. Assuming that $V_{\mathbf{kq}}$ connects $|n\mathbf{k}\rangle$ state only to nondegenerate ones, this approach gives $\varepsilon_{n,\mathbf{k}+\mathbf{q}} = \varepsilon_{n\mathbf{k}} + \langle n\mathbf{k}|V_{\mathbf{kq}}|n\mathbf{k}\rangle + \sum' |\langle n\mathbf{k}|V_{\mathbf{kq}}|n'\mathbf{k}'\rangle|^2/(\varepsilon_{n\mathbf{k}} - \varepsilon_{n'\mathbf{k}'}) + \cdots$. In principle, $\sum' \equiv \sum_{\{n'\mathbf{k}'\}\neq\{n\mathbf{k}\}}$ sums over all of the nondegenerate quantum states, but it is sufficient to keep only the interband terms with $\mathbf{k}' = \mathbf{k}$ in the small-$\mathbf{q}$ limit. By matching the coefficients of the linear and quadratic terms in $\mathbf{q}$, we eventually identify $\hbar v_{n\mathbf{k}}^i = \langle n\mathbf{k}|\partial H_{\mathbf{k}}/\partial k_i|n\mathbf{k}\rangle = \partial\varepsilon_{n\mathbf{k}}/\partial k_i$ as the effective band velocity and

$$\left[\mathbb{M}_{n\mathbf{k}}^{-1}\right]^{ij} = \frac{1}{\hbar^2}\langle n\mathbf{k}|\frac{\partial^2 H_{\mathbf{k}}}{\partial k_i\partial k_j}|n\mathbf{k}\rangle + 2\,\mathrm{Re}\sum{}' \frac{\langle n\mathbf{k}|\frac{\partial H_{\mathbf{k}}}{\partial k_i}|n'\mathbf{k}\rangle\langle n'\mathbf{k}|\frac{\partial H_{\mathbf{k}}}{\partial k_j}|n\mathbf{k}\rangle}{\hbar^2(\varepsilon_{n\mathbf{k}} - \varepsilon_{n'\mathbf{k}})} \quad (1)$$

as the inverse effective-band-mass tensor of the particle for the $\mathbf{k}$ state. Here Re denotes the real part of the resultant summation. In Eq. (1), while the first term on the right-hand side is due precisely to the intraband contribution $[\mathrm{m}_{n\mathbf{k}}^{-1}]^{ij}$ to the effective inverse mass tensor of the corresponding energy band, the second term is generated by the $\mathbf{q}$-induced virtual interband processes.

Despite the use of perturbation theory in its derivation, Eq. (1) is exact and in principle the interband contribution need not necessarily be a small correction to the intraband one. For instance, one can alternatively obtain Eq. (1) by taking the derivatives of the wave equation $H_{\mathbf{K}}|n\mathbf{K}\rangle = \varepsilon_{n\mathbf{K}}|n\mathbf{K}\rangle$ with respect to $\mathbf{K} = \mathbf{k} + \mathbf{q}$ as follows. Using the orthonormalization condition $\langle n\mathbf{K}|n'\mathbf{K}'\rangle = \delta_{nn'}\delta(\mathbf{K} - \mathbf{K}')$ for the $\mathbf{K}$ subspace of energy eigenstates, where $\delta_{nn'}$ is a Kronecker delta and $\delta(x)$ is a Dirac delta function, we first obtain $\langle n\mathbf{K}|\partial H_{\mathbf{K}}/\partial K_i|n'\mathbf{K}'\rangle = (\varepsilon_{n\mathbf{K}} - \varepsilon_{n'\mathbf{K}'})(\partial\langle n\mathbf{K}|/\partial K_i)|n'\mathbf{K}'\rangle + (\partial\varepsilon_{n\mathbf{K}}/\partial K_i)\delta_{nn'}\delta(\mathbf{K} - \mathbf{K}')$, leading to $\partial\varepsilon_{n\mathbf{K}}/\partial K_i = \langle n\mathbf{K}|\partial H_{\mathbf{K}}/\partial K_i|n\mathbf{K}\rangle$. Then, by taking the derivative of this expression with respect to K_j, i.e., $\partial^2\varepsilon_{n\mathbf{K}}/\partial K_i\partial K_j = \langle n\mathbf{K}|\partial^2 H_{\mathbf{K}}/\partial K_i\partial K_j|n\mathbf{K}\rangle + (\partial\langle n\mathbf{K}|/\partial K_j)|\partial H_{\mathbf{K}}/\partial K_i|n\mathbf{K}\rangle + \langle n\mathbf{K}|\partial H_{\mathbf{K}}/\partial K_i|(\partial|n\mathbf{K}\rangle/\partial K_j)$, and using the completeness relation $\mathbb{I} = \sum_{n\mathbf{K}}|n\mathbf{K}\rangle\langle n\mathbf{K}|$ together with the derivative of the orthonormalization condition $(\partial\langle n\mathbf{K}|/\partial K_i)|n'\mathbf{K}\rangle + \langle n\mathbf{K}|(\partial|n'\mathbf{K}\rangle/\partial K_i) = 0$ for the $\mathbf{K}$ subspace of interest, we eventually arrive at

$$\frac{\partial^2\varepsilon_{n\mathbf{K}}}{\partial K_i\partial K_j} = \langle n\mathbf{K}|\frac{\partial^2 H_{\mathbf{K}}}{\partial K_i\partial K_j}|n\mathbf{K}\rangle + 2\,\mathrm{Re}\sum{}'(\varepsilon_{n\mathbf{K}} - \varepsilon_{n'\mathbf{K}'}) \times \frac{\partial\langle n\mathbf{K}|}{\partial K_i}|n'\mathbf{K}'\rangle\langle n'\mathbf{K}'|\frac{\partial|n\mathbf{K}\rangle}{\partial K_j}. \quad (2)$$

This expression corresponds precisely to the coefficient $\hbar^2[\mathbb{M}_{n\mathbf{k}}^{-1}]^{ij}$ of the quadratic term when $\mathbf{q}\to\mathbf{0}$, producing Eq. (1) without the use of perturbative approach.

Having established the theoretical framework of the effective-band-mass theorem for multiband Hamiltonians, next we focus on two-band systems for their simplicity and not only highlight the intriguing interpretation of the interband contribution from the quantum geometrical perspective but also illustrate its relative importance for a number of toy models that are of immediate experimental and/or theoretical interest.

III. QUANTUM METRIC OF THE PROJECTED HILBERT SPACE

For this purpose, we note that the interband contribution to the effective-band-mass theorem given in Eq. (1) resembles closely, but is not quite exactly, the quantum metric $g_{n\mathbf{k}}^{ij}$ of the corresponding energy eigenstate. Recall that [37–39] $g_{n\mathbf{k}}^{ij} = \mathrm{Re}(\partial\langle n\mathbf{k}|/\partial k_i)(\sum' |n'\mathbf{k}'\rangle\langle n'\mathbf{k}'|)(\partial|n\mathbf{k}\rangle/\partial k_j)$ is defined as the real part of the so-called quantum geometric tensor $Q_{n\mathbf{k}}^{ij} = g_{n\mathbf{k}}^{ij} - (i/2)F_{n\mathbf{k}}^{ij}$ of the projected Hilbert space, which can be equivalently expressed as $g_{n\mathbf{k}}^{ij} = \sum_{\mathbf{k}'} g_{n\mathbf{k}\mathbf{k}'}^{ij}$, where

$$g_{n\mathbf{k}\mathbf{k}'}^{ij} = \mathrm{Re}\sum{}' \frac{\langle n\mathbf{k}|\frac{\partial H_{\mathbf{k}}}{\partial k_i}|n'\mathbf{k}'\rangle\langle n'\mathbf{k}'|\frac{\partial H_{\mathbf{k}}}{\partial k_j}|n\mathbf{k}\rangle}{(\varepsilon_{n\mathbf{k}} - \varepsilon_{n'\mathbf{k}'})^2}. \quad (3)$$

Since only the interband terms with $\mathbf{k}' = \mathbf{k}$ survive in Eq. (1) or (2), we have $g_{n\mathbf{k}}^{ij} \equiv g_{n\mathbf{k}\mathbf{k}}^{ij}$ in this paper. The geometrical importance of the quantum metric reveals itself as a measure of the quantum distance between differing quantum states, i.e., $ds_n^2 = |\langle n\mathbf{k}|n\mathbf{k}\rangle|^2 - |\langle n\mathbf{k}|n, \mathbf{k} + d\mathbf{k}\rangle|^2 = \sum_{ij} g_{n\mathbf{k}}^{ij} dk_i dk_j$. In contrast, the imaginary part $F_{n\mathbf{k}}^{ij}$ of the quantum geometric tensor is the Berry curvature, i.e., it is a distinct but related quantity corresponding to the emergent magnetic field in $\mathbf{k}$ space.

Even though both $g_{n\mathbf{k}}^{ij}$ and $F_{n\mathbf{k}}^{ij}$ characterize the local $\mathbf{k}$-space geometry of the underlying quantum states, they may also be linked to the global properties of the system in somewhat peculiar ways. For instance, the topological Chern invariant of a quantum Hall system is determined by an integration of $F_{n\mathbf{k}}^{ij}$ in $\mathbf{k}$ space, i.e., $2\pi C_n = \int_{BZ} dk_x dk_y F_{n\mathbf{k}}^{xy}$ controls the Hall conductivity [39]. Likewise, the superfluid density of some flat-band and two-band superfluids, which exhibit nontrivial quantum geometry, has a substantial contribution determined by an integration of $g^{ij}_{n\mathbf{k}}$ with a proper weight factor [31–33,35]. Furthermore, by showing that the quantum metric contribution accounts for a sizeable fraction of the (Cooper) pair mass throughout the BCS-BEC crossover [33,34], we have revealed the physical origin of its governing role in the superfluid density and hinted at its plausible roles in many other observables including the sound velocity and spin susceptibility [36]. Next we point out a distinct but related effect on the effective band mass of a single particle near the band minimum of the lower helicity band.

IV. EFFECTIVE-BAND-MASS THEOREM FOR TWO-BAND HAMILTONIANS

We consider a generic two-band Hamiltonian density $H_\mathbf{k}$ and parametrize its energy eigenstates and eigenvalues with $|s\mathbf{k}\rangle$ and $\varepsilon_{s\mathbf{k}} = \epsilon_\mathbf{k} + s d_\mathbf{k}$, respectively. Here $s = +$ ($s = -$) labels the upper (lower) bands that are separated by a $\mathbf{k}$-dependent energy gap of $2d_\mathbf{k}$. When the geometric response is due only to the intermediate states from the differing band, i.e., $V_{\mathbf{kq}}$ connects $|s\mathbf{k}\rangle$ to $|-s,\mathbf{k}\rangle$ with $d_\mathbf{k} \neq 0$, a compact way to express the resultant effective-band-mass theorem for such a two-band system is

$$\left[\mathbb{M}^{-1}_{s\mathbf{k}}\right]^{ij} = \left[\mathrm{m}^{-1}_{s\mathbf{k}}\right]^{ij} + \frac{2s}{\hbar^2} d_\mathbf{k} g^{ij}_\mathbf{k}. \quad (4)$$

Here the intraband contribution is simply denoted by $[\mathrm{m}^{-1}_{s\mathbf{k}}]^{ij}$, but the interband one is directly controlled by the total quantum metric $g^{ij}_\mathbf{k} = \sum_s g^{ij}_{s\mathbf{k}} = \mathrm{Re}\sum_s (\partial\langle s\mathbf{k}|/\partial k_i)(|-s,\mathbf{k}\rangle\langle -s,\mathbf{k}|)(\partial|s\mathbf{k}\rangle/\partial k_j)$ of the corresponding quantum state. Note that the interband contributions have opposite signs for the $s = \pm$ bands. For the isotropic directions of interest in this paper, the relevant effective mass is defined as the $\mathbf{k}$-space average of Eq. (4) over the degenerate subspace.

To illustrate the relative importance of the interband contribution, next we consider a single spin-$\frac{1}{2}$ particle that is described by the generic Hamiltonian density $H_\mathbf{k} = \epsilon_\mathbf{k}\sigma_0 + \mathbf{d}_\mathbf{k}\cdot\boldsymbol{\sigma}$, where $\epsilon_k = \hbar^2k^2/2m_0$ is the usual free-particle dispersion with m_0 the bare mass and $\mathbf{d}_\mathbf{k} = \sum_i d^i_\mathbf{k}\hat{\boldsymbol{i}}$ is the SOC field with $\hat{\boldsymbol{i}}$ the unit vector along the i direction. Here σ_0 is a 2×2 identity matrix and $\boldsymbol{\sigma} = \sum_i \sigma_i\hat{\boldsymbol{i}}$ is a vector of Pauli spin matrices in such a way that $d^i_\mathbf{k} = \hbar\alpha_i k_i$ corresponds to the Weyl SOC when $\alpha_i = \alpha$ for all $i = \{x, y, z\}$, a Rashba SOC when $\alpha_z = 0$, and an equal Rashba-Dresselhaus (ERD) SOC when $\alpha_y = \alpha_z = 0$. Here we choose $\alpha \geqslant 0$ without loss of generality. Note that $\varepsilon_{s\mathbf{k}} = \epsilon_\mathbf{k} + s d_\mathbf{k}$ is the s-helicity dispersion with the energy eigenstate $|s\mathbf{k}\rangle^\mathrm{T} = (-d^x_\mathbf{k} + \mathrm{i}d^y_\mathbf{k}, d^z_\mathbf{k} - s d_\mathbf{k})/\sqrt{2d_\mathbf{k}(d_\mathbf{k} - s d^z_\mathbf{k})}$, where $d_\mathbf{k} = |\mathbf{d}_\mathbf{k}|$ and T is the transpose operator. The quantum geometry is trivial for the ERD SOC as $g^{ij}_{s\mathbf{k}} = 0$ for the entire $\mathbf{k}$ space. It turns out that the quantum metrics of the $s = \pm$ bands are equal and their sum can be expressed as $g^{ij}_\mathbf{k} = (\partial\hat{\boldsymbol{d}}_\mathbf{k}/\partial k_i)\cdot(\partial\hat{\boldsymbol{d}}_\mathbf{k}/\partial k_j)/2$, where $\hat{\boldsymbol{d}}_\mathbf{k} = \mathbf{d}_\mathbf{k}/d_\mathbf{k}$ is the unit vector along the SOC field. The equivalent expression $g^{ij}_\mathbf{k} = [\sum_\ell(\partial d^\ell_\mathbf{k}/\partial k_i)(\partial d^\ell_\mathbf{k}/\partial k_j) - (\partial d_\mathbf{k}/\partial k_i)(\partial d_\mathbf{k}/\partial k_j)]/2d^2_\mathbf{k}$ reduces simply to $g^{ij}_\mathbf{k} = \hbar^2\alpha_i\alpha_j(d^2_\mathbf{k}\delta_{ij} - d^i_\mathbf{k}d^j_\mathbf{k})/2d^4_\mathbf{k}$, showing that $g^{ij}_\mathbf{k} = 0$ in general for all $\mathbf{k}$ states unless $\alpha_i\alpha_j \neq 0$.

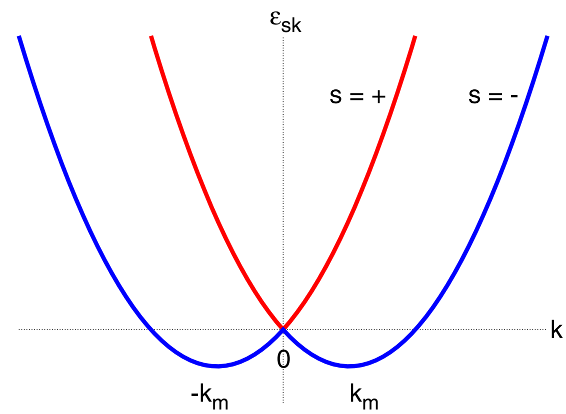

FIG. 1. By breaking the spin degeneracy of the particle dispersions $\epsilon_{\sigma\mathbf{k}} = \epsilon_\mathbf{k}$, the SOC $\mathbf{d}_\mathbf{k}\cdot\boldsymbol{\sigma}$ creates a pair of helicity bands $\varepsilon_{s\mathbf{k}} = \epsilon_\mathbf{k} + s d_\mathbf{k}$. Here $s = +$ ($s = -$) corresponds to the upper (lower) branches, illustrated for a free particle $\epsilon_k = \hbar^2k^2/2m_0$ with the Weyl SOC $d_k = \hbar\alpha k$. We are interested in the effective band mass of the particle near the band minimum $\mathbf{k_m}$ of the lower helicity band.

In Eq. (4), the intraband contribution $m_{sk} = m_0$ is already isotropic in $\mathbf{k}$ space and we take the angular average of the geometric contribution over the degenerate direction, i.e., $\langle g^{ij}_\mathbf{k}\rangle = g_k\delta_{ij}$ with $g_k = \hbar^2\alpha^2(D-1)/2Dd^2_k$. Here $D = 3$ for the radial direction of Weyl SOC with $d_k = \hbar\alpha k$, $D = 2$ for the polar direction of Rashba SOC with $d_k = \hbar\alpha k_\perp$, and $D = 1$ for the q_x direction of ERD SOC with $d_k = \hbar\alpha|k_x|$. This leads to

$$\frac{M_{sk}}{m_0} = \frac{Dd_k}{Dd_k + s(D-1)m_0\alpha^2} \quad (5)$$

for the angular average $\langle[\mathbb{M}^{-1}_{s\mathbf{k}}]^{ij}\rangle = \delta_{ij}/M_{sk}$ of the effective-mass theorem, showing that the geometric contribution is negligible at large momentum, i.e., when $Dd_k \gg (D-1)m_0\alpha^2$. In this paper, we are interested in the effective band mass of the particle near the band minimum $\mathbf{k_m}$ of the lower helicity band; see, e.g., the Weyl SOC illustrated in Fig. 1. Plugging $k_m = m_0\alpha/\hbar$ in Eq. (5), we find

$$M_{-,k_m} = Dm_0, \quad (6)$$

where D is the dimensionality of the isotropic SOC field.

This analysis implies that the interband contribution to the effective band mass of the particle is a nonperturbative one for both Weyl and Rashba SOCs. In addition, this contribution is clearly independent of α at the band minimum as long as $\alpha \neq 0$. Furthermore, the dimensionality of the $\mathbf{k}$ space does not play any role for the Rashba SOC, i.e., $M^\perp_{-,k_m} = 2m_0$ in both two and three dimensions. No matter how bizarre these results sound, we note that they are consistent with the effective mass M_{tb} of the relevant two-body bound states reported in the Fermi gas literature [41–49], where the binding occurs between an $(\uparrow;\mathbf{k}+\mathbf{q}/2)$ particle and a $(\downarrow;-\mathbf{k}+\mathbf{q}/2)$ one in the presence of a contact attraction. For instance, in Fig. 2 we reproduce the xx component M^{xx}_{tb} as a function of the two-body binding energy E_{tb} in vacuum. In the noninteracting limit when $E_{tb} \to 0^+$, we clearly see that $M_{tb} = 6m_0$ is isotropic in space for the Weyl SOC and $M^\perp_{tb} = 4m_0$ is

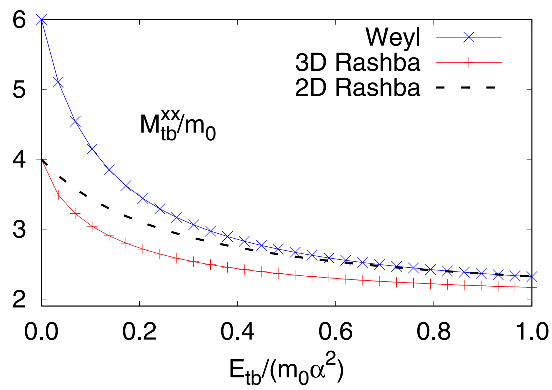

FIG. 2. The xx component of the effective mass of the two-body bound state M_{tb}^{xx} is shown for the Weyl and Rashba SOCs as a function of the two-body binding energy E_{tb} in vacuum [41–49]. In the noninteracting limit when $E_{tb} \to 0^+$, we note that M_{tb}^{xx} approaches twice the effective band mass of the particle at the band minimum of its lower helicity band, i.e., $M_{tb} \to 2M_{-,k_m}$, in all cases considered here.

isotropic in the xy plane for the Rashba SOC as long as $\alpha \neq 0$, independently of its magnitude. In addition, it is also known that $M_{tb}^{zz} = 2m_0$ along the z direction for the Rashba SOC in three dimensions and that the ERD SOC has no effect on the two-body problem. Thus, as M_{tb} coincides with twice the effective band mass of the particle at the band minimum of its lower helicity band, the geometric mass enhancement uncovers the mystery behind M_{tb} in the noninteracting limit. When E_{tb} increases from 0, however, a competing but distinct geometric effect on the bound state reduces M_{tb} towards the expected value $2m_0$ in the $E_{tb} \gg m_0\alpha^2$ limit [34].

We note in passing that the electronic properties of some graphenelike solid-state materials are well described by the low-energy Hamiltonian density $H_{\mathbf{k}} = \hbar\alpha\mathbf{k}\cdot\boldsymbol{\sigma}$, where α refers to the Fermi velocity and $\boldsymbol{\sigma}$ refers not to the spin degrees of freedom of the electron but to the sublattice degrees of freedom of the underlying crystal (i.e., honeycomb) lattice [14]. Since the helicity dispersions $\varepsilon_{sk} = s\alpha k$ are isotropic and linear in $\mathbf{k}$ space, the intraband contribution to the inverse effective mass vanishes, suggesting that the effective band mass M_{sk} is determined solely by the interband contribution. Thus, setting $m_0 \to \infty$ in Eq. (5), we find a linearly dispersing effective band mass

$$M_{sk} = \frac{sD}{D-1}\frac{\hbar k}{\alpha} \tag{7}$$

for the particles (holes) in the upper (lower) helicity bands, where $D \geqslant 2$ is the dimensionality of the $\mathbf{k}$ space. Indeed, the long-established realization that the effective cyclotron mass $M_{sc} = s\hbar k_F/\alpha$ of the charge carriers in graphene has a strong $\sqrt{\rho}$ dependence in the low-density limit provided early smoking-gun evidence for the existence of a massless Dirac quasiparticle in the $k \to 0^+$ limit [12–14]. Here $\rho = k_F^2/\pi$ is the electronic density of graphene with k_F the Fermi wave vector.

V. CONCLUSION

In summary, our so-called effective-band-mass theorem for the helicity bands has two physically distinct components: In addition to the usual contribution coming from the intraband processes, there exists a geometric contribution stemming from the virtual interband ones. It turns out that the latter contribution is directly controlled by the quantum metric of the corresponding quantum state. To illustrate the relative importance of the interband contribution, we considered a spin-orbit-coupled spin-$\frac{1}{2}$ particle and calculated its effective band mass at the band minimum of the lower helicity band. We found that the bare mass m_0 of the particle jumps to $2m_0$ for the Rashba coupling and to $3m_0$ for the Weyl coupling, independently of the coupling strength. We argued that such a geometric enhancement of the effective mass of the particle is consistent with the effective mass of the relevant two-body bound state in the noninteracting limit [41–49]. In addition, for graphenelike solid-state materials, we noted that the physical mechanism behind the linearly dispersing effective cyclotron mass of a Dirac quasiparticle [12–14] may be interpreted as a geometric mass acquisition.

ACKNOWLEDGMENTS

The author thanks F. M. Ramazanoğlu and M. Ö. Oktel for critical reading of the manuscript and acknowledges support from TÜBİTAK and the BAGEP award of the Turkish Science Academy.

[1] Y.-J. Lin, K. Jiménez-García, and I. B. Spielman, Spin-orbit-coupled Bose-Einstein condensates, Nature (London) **471**, 83 (2011).
[2] J.-Y. Zhang, S.-C. Ji, Z. Chen, L. Zhang, Z.-D. Du, B. Yan, G.-S. Pan, B. Zhao, Y.-J. Deng, H. Zhai, S. Chen, and J.-W. Pan, Collective Dipole Oscillations of a Spin-Orbit Coupled Bose-Einstein Condensate, Phys. Rev. Lett. **109**, 115301 (2012).
[3] P. Wang, Z.-Q. Yu, Z. Fu, J. Miao, L. Huang, S. Chai, H. Zhai, and J. Zhang, Spin-Orbit Coupled Degenerate Fermi Gases, Phys. Rev. Lett. **109**, 095301 (2012).
[4] L. W. Cheuk, A. T. Sommer, Z. Hadzibabic, T. Yefsah, W. S. Bakr, and M. W. Zwierlein, Spin-Injection Spectroscopy of a Spin-Orbit Coupled Fermi Gas, Phys. Rev. Lett. **109**, 095302 (2012).
[5] C. Qu, C. Hamner, M. Gong, C. Zhang, and P. Engels, Observation of zitterbewegung in a spin-orbit-coupled Bose-Einstein condensate, Phys. Rev. A **88**, 021604(R) (2013).
[6] A. J. Olson, S.-J. Wang, R. J. Niffenegger, C.-H. Li, C. H. Greene, and Y. P. Chen, Tunable Landau-Zener transitions in a spin-orbit-coupled Bose-Einstein condensate, Phys. Rev. A **90**, 013616 (2014).
[7] K. Jiménez-García, L. J. LeBlanc, R. A. Williams, M. C. Beeler, C. Qu, M. Gong, C. Zhang, and I. B. Spielman, Tunable Spin-Orbit Coupling via Strong Driving in Ultracold-Atom Systems, Phys. Rev. Lett. **114**, 125301 (2015).

[8] L. Huang, Z. Meng, P. Wang, P. Peng, S.-L. Zhang, L. Chen, D. Li, Q. Zhou, and J. Zhang, Experimental realization of a two-dimensional synthetic spin-orbit coupling in ultracold Fermi gases, Nat. Phys. **12**, 540 (2016).
[9] Z. Meng, L. Huang, P. Peng, D. Li, L. Chen, Y. Xu, C. Zhang, P. Wang, and J. Zhang, Experimental Observation of a Topological Band Gap Opening in Ultracold Fermi Gases with Two-Dimensional Spin-Orbit Coupling, Phys. Rev. Lett. **117**, 235304 (2016).
[10] Z. Wu, L. Zhang, W. Sun, X.-T. Xu, B.-Z. Wang, S.-C. Ji, Y. Deng, S. Chen, X.-J. Liu, and J.-W. Pan, Realization of two-dimensional spin-orbit coupling for Bose-Einstein condensates, Science **354**, 83 (2016).
[11] W. Sun, B.-Z. Wang, X.-T. Xu, C.-R. Yi, L. Zhang, Z. Wu, Y. Deng, X.-J. Liu, S. Chen, and J.-W. Pan, Long-Lived 2D Spin-Orbit Coupled Topological Bose Gas, Phys. Rev. Lett. **121**, 150401 (2018).
[12] K. S. Novoselov, A. K. Geim, S. V. Morozov, D. Jiang, M. I. Katsnelson, I. V. Grigorieva, S. V. Dubonos, and A. A. Firsov, Two-dimensional gas of massless Dirac fermions in graphene, Nature (London) **438**, 197 (2005).
[13] Y. Zhang, Y.-W. Tan, H. L. Stormer, and P. Kim, Experimental observation of the quantum Hall effect and Berry's phase in graphene, Nature (London) **438**, 201 (2005).
[14] A. H. Castro Neto, F. Guinea, N. M. R. Peres, K. S. Novoselov, and A. K. Geim, The electronic properties of graphene, Rev. Mod. Phys. **81**, 109 (2009).
[15] M. Z. Hasan and C. L. Kane, Colloquium: Topological insulators, Rev. Mod. Phys. **82**, 3045 (2010).
[16] X.-L. Qi and S.-C. Zhang, Topological insulators and superconductors, Rev. Mod. Phys. **83**, 1057 (2011).
[17] A. Kobayashi, S. Katayama, Y. Suzumura, and H. Fukuyama, Massless fermions in organic conductor, J. Phys. Soc. Jpn. **76**, 034711 (2007).
[18] L. Tarruell, D. Greif, T. Uehlinger, G. Jotzu, and Tilman Esslinger, Creating, moving and merging Dirac points with a Fermi gas in a tunable honeycomb lattice, Nature (London) **483**, 302 (2012).
[19] K. K. Gomes, W. Mar, W. Ko, F. Guinea, and H. C. Manoharan, Designer Dirac fermions and topological phases in molecular graphene, Nature (London) **483**, 306 (2012).
[20] M. Bellec, U. Kuhl, G. Montambaux, and F. Mortessagne, Topological Transition of Dirac Points in a Microwave Experiment, Phys. Rev. Lett. **110**, 033902 (2013).
[21] N. Marzari and D. Vanderbilt, Maximally localized generalized Wannier functions for composite energy bands, Phys. Rev. B **56**, 12847 (1997).
[22] P. Zanardi, P. Giorda, and M. Cozzini, Information-Theoretic Differential Geometry of Quantum Phase Transitions, Phys. Rev. Lett. **99**, 100603 (2007).
[23] F. D. M. Haldane, Geometrical Description of the Fractional Quantum Hall Effect, Phys. Rev. Lett. **107**, 116801 (2011).
[24] T. Neupert, C. Chamon, and C. Mudry, Measuring the quantum geometry of Bloch bands with current noise, Phys. Rev. B **87**, 245103 (2013).
[25] T. S. Jackson, G. Moller, and R. Roy, Geometric stability of topological lattice phases, Nat. Commun. **6**, 8629 (2015).
[26] Y. Gao, S. A. Yang, and Q. Niu, Field Induced Positional Shift of Bloch Electrons and Its Dynamical Implications, Phys. Rev. Lett. **112**, 166601 (2014).
[27] M. Claassen, C. H. Lee, R. Thomale, X.-L. Qi, and T. P. Devereaux, Position-Momentum Duality and Fractional Quantum Hall Effect in Chern Insulators, Phys. Rev. Lett. **114**, 236802 (2015).
[28] A. Srivastava and A. Imamoglu, Signatures of Bloch-Band Geometry on Excitons: Nonhydrogenic Spectra in Transition-Metal Dichalcogenides, Phys. Rev. Lett. **115**, 166802 (2015).
[29] F. Piéchon, A. Raoux, J.-N. Fuchs, and G. Montambaux, Geometric orbital susceptibility: Quantum metric without Berry curvature, Phys. Rev. B **94**, 134423 (2016).
[30] T. Ozawa, Steady-state Hall response and quantum geometry of driven-dissipative lattices, Phys. Rev. B **97**, 041108(R) (2018).
[31] S. Peotta and P. Törmä, Superfluidity in topologically nontrivial flat bands, Nat. Commun. **6**, 8944 (2015).
[32] A. Julku, S. Peotta, T. I. Vanhala, D.-H. Kim, and P. Törmä, Geometric Origin of Superfluidity in the Lieb-Lattice Flat Band, Phys. Rev. Lett. **117**, 045303 (2016).
[33] M. Iskin, Berezinskii-Kosterlitz-Thouless transition in the time-reversal-symmetric Hofstadter-Hubbard model, Phys. Rev. A **97**, 013618 (2018).
[34] M. Iskin, Quantum metric contribution to the pair mass in spin-orbit coupled Fermi superfluids, Phys. Rev. A **97**, 033625 (2018).
[35] M. Iskin, Exposing the quantum geometry of spin-orbit coupled Fermi superfluids, Phys. Rev. A **97**, 063625 (2018).
[36] M. Iskin, Spin-susceptibility of spin-orbit coupled Fermi superfluids, Phys. Rev. A **97**, 053613 (2018).
[37] J. P. Provost and G. Vallee, Riemannian structure on manifolds of quantum states, Commun. Math. Phys. **76**, 289 (1980).
[38] M. V. Berry, *The Quantum Phase, Five Years after in Geometric Phases in Physics*, edited by A. Shapere and F. Wilczek (World Scientific, Singapore, 1989).
[39] D. J. Thouless, *Topological Quantum Numbers in Nonrelativistic Physics* (World Scientific, Singapore, 1998).
[40] N. W. Ashcroft and N. D. Mermin, *Solid State Physics*, 1st ed. (Harcourt, New York, 1976).
[41] Z.-Q. Yu and H. Zhai, Spin-Orbit Coupled Fermi Gases across a Feshbach Resonance, Phys. Rev. Lett. **107**, 195305 (2011).
[42] M. Iskin and A. L. Subaşı, Quantum phases of atomic Fermi gases with anisotropic spin-orbit coupling, Phys. Rev. A **84**, 043621 (2011).
[43] L. Jiang, X.-J. Liu, H. Hu, and H. Pu, Rashba spin-orbit-coupled atomic Fermi gases, Phys. Rev. A **84**, 063618 (2011).
[44] H. Hu, L. Jiang, X.-J. Liu, and H. Pu, Probing Anisotropic Superfluidity in Atomic Fermi Gases with Rashba Spin-Orbit Coupling, Phys. Rev. Lett. **107**, 195304 (2011).
[45] L. He and X.-G. Huang, BCS-BEC Crossover in 2D Fermi Gases with Rashba Spin-Orbit Coupling, Phys. Rev. Lett. **108**, 145302 (2012).
[46] L. He and X.-G. Huang, BCS-BEC crossover in three-dimensional Fermi gases with spherical spin-orbit coupling, Phys. Rev. B **86**, 014511 (2012).
[47] J. P. Vyasanakere and V. B. Shenoy, Rashbons: Properties and their significance, New J. Phys. **14**, 043041 (2012).
[48] J. P. Vyasanakere and V. B. Shenoy, Collective excitations, emergent Galilean invariance, and boson-boson interactions across the BCS-BEC crossover induced by a synthetic Rashba spin-orbit coupling, Phys. Rev. A **86**, 053617 (2012).
[49] Noting that the band minimum of the lower helicity band is locally flat for all $\mathbf{k_m}$ states, our results are also consistent with

that of P. Törmä, L. Liang, and S. Peotta, Quantum metric and effective mass of a two-body bound state in a flat band, Phys. Rev. B **98**, 220511(R) (2018). For an energetically isolated flat band in $\mathbf{k}$ space, the inverse mass tensor of the two-body bound state is reported as $\hbar^2[\mathbb{M}_{tb}^{-1}]^{ij} = |E_0|\langle g_{\mathbf{k}}^{ij}\rangle$, where $E_0 = -U/2$ is the energy of the zero-momentum pair with $U \leqslant 0$ characterizing the short-range attractive interactions and $\langle g_{\mathbf{k}}^{ij}\rangle = (1/N)\sum_{\mathbf{k}} g_{\mathbf{k}}^{ij}$ is an average over the entire $\mathbf{k}$ space with N degenerate points. In connection to our case, reexpressing the average effective mass as $\hbar^2\langle[\mathbb{M}_{-,\mathbf{k_m}}^{-1}]^{ij}\rangle = \hbar^2\delta_{ij}/m_0 - 2m_0\alpha^2\langle g_{\mathbf{k_m}}^{ij}\rangle$, we directly identify the average $|E_0|\langle g_{\mathbf{k_m}}^{ij}\rangle$ over the degenerate subspace as the geometric contribution to the inverse pair mass tensor, where $E_0 = -m_0\alpha^2$ is the energy of the zero-momentum pair. See [34] for a similar observation and note [50].

[50] For the isotropic directions of interest in this paper, we define the relevant effective mass as the $\mathbf{k}$-space average of Eq. (4) over the degenerate subspace. Such an average mass may also be motivated by the electrical conductivity tensor $\boldsymbol{\sigma}_n^{ij}$. For instance, within the semiclassical Boltzmann transport equation, integrating the tensor $\boldsymbol{\sigma}_n^{ij} \propto \sum_{\mathbf{k}} v_{n\mathbf{k}}^i v_{n\mathbf{k}}^j[-\partial f(\varepsilon_{n\mathbf{k}} - \mu)/\partial\varepsilon]$ by parts, we may reexpress it as $\boldsymbol{\sigma}_n^{ij} \propto \sum_{\mathbf{k}}[\mathbb{M}_{n\mathbf{k}}^{-1}]^{ij} f(\varepsilon_{n\mathbf{k}} - \mu)$. Here $f(x) = 1/[e^{x/k_BT} + 1]$ is the Fermi-Dirac distribution, with k_B the Boltzmann constant and T the temperature, and μ is the chemical potential. See [40], p. 250 for details.